remote sensing

MDPI

Article

Exploring the Potential of OpenStreetMap Data in Regional Economic Development Evaluation Modeling

Zhe Wang [1], Jianghua Zheng [1,2,*], Chuqiao Han [1], Binbin Lu [1,3], Danlin Yu [4], Juan Yang [1] and Linzhi Han [5]

[1] College of Geographical and Remote Sensing Science, Xinjiang University, Urumqi 830046, China; 107552101073@stu.xju.edu.cn (Z.W.); hanchuqiao@stu.xju.edu.cn (C.H.); binbinlu@whu.edu.cn (B.L.); yangjuan@stu.xju.edu.cn (J.Y.)
[2] Key Lab of Smart City and Environmental Modelling, Xinjiang University, Urumqi 830046, China
[3] School of Remote Sensing and Information Engineering, Wuhan University, Wuhan 430079, China
[4] Department of Earth and Environmental Studies, Montclair State University, Montclair, NJ 07043, USA; yud@mail.montclair.edu
[5] School of Economics and Management, Xinjiang University, Urumqi 830046, China; hanlinzhi@xju.edu.cn
* Correspondence: zheng.jianghua@xju.edu.cn

Abstract: In regional development studies, GDP serves as an important indicator for evaluating the developing levels of a region. However, due to statistical methods and possible human-induced interfering factors, GDP is also a commonly criticized indicator for less accurately assessing regional economic development in a dynamic environment, especially during a globalized era. Moreover, common data collection approaches are often challenging to obtain in real-time, and the assessments are prone to inaccuracies. This is especially true in economically underdeveloped regions where data are often less frequently or accurately collected. In recent years, Nighttime Light (NTL) data have emerged as a crucial supplementary data source for regional economic development evaluation and analysis. We adapt this approach and attempt to integrate multiple sources of spatial data to provide a new perspective and more effective tools for economic development evaluation. In our current study, we explore the integration of OpenStreetMap (OSM) data and NTL data in regional studies, and apply a Geographically and Temporally Weighted Regression model (GTWR) for modeling and evaluating regional economic development. Our results suggest that: (1) when using OSM data as a single data source for economic development evaluation, the adjusted R^2 value is 0.889. When using NTL data as a single data source for economic development evaluation, the adjusted R^2 value is 0.911. However, the fitting performance of OSM data with GDP shows a gradual improvement over time, while the fitting performance of NTL data exhibits a gradual decline starting from the year 2014; (2) Among the economic evaluation models, the GTWR model demonstrates the highest accuracy with an AICc value of 49,112.71, which is 2750.94 lower than the ordinary least squares (OLS) model; (3) The joint modeling of OSM data with NTL data yields an adjusted R^2 value of 0.956, which is higher than using either one of them alone. Moreover, this joint modeling approach demonstrates excellent fitting performance, particularly in economically underdeveloped regions, providing a potential alternative for development evaluation in data-poor regions.

Keywords: OpenStreetMap (OSM); nighttime light (NTL); gross domestic product (GDP); geographically and temporally weighted regression (GTWR); China

Citation: Wang, Z.; Zheng, J.; Han, C.; Lu, B.; Yu, D.; Yang, J.; Han, L. Exploring the Potential of OpenStreetMap Data in Regional Economic Development Evaluation Modeling. *Remote Sens.* **2024**, *16*, 239. https://doi.org/10.3390/rs16020239

Academic Editor: Desheng Liu

Received: 26 November 2023
Revised: 2 January 2024
Accepted: 5 January 2024
Published: 8 January 2024

1. Introduction

Economic development evaluation is the process of assessing and analyzing the economic conditions and developmental level of a country or region. This evaluation not only provides a reference and guidance for achieving United Nations Sustainable Development Goal 10 (SDG-10) [1], which aims to reduce inequality within and between countries, but also holds significant importance in promoting sustainable economic development, enhancing economic competitiveness, and improving the country's image and creditworthiness [2–4]. In

the process of achieving sustainable development goals, economic development evaluation plays a crucial role in eliminating poverty, promoting social justice, enhancing education levels, and improving environmental quality, among other aspects [5–10]. In addition, economic development evaluation also serves as the foundation for policymakers to formulate and implement measures and policies. Economic development assessment is therefore one of the important tools for promoting economic and social progress and has far-reaching implications for achieving the Sustainable Development Goals.

China, as the world's second-largest economy, has achieved tremendous economic development accomplishments in the past few decades. However, there are significant disparities in the economic development levels and patterns among different regions and prefecture-level cities [11]. At present, GDP is the most widely used economic indicator and standard in economic development evaluation [12,13]. However, the calculation of GDP heavily relies on the official statistical agencies of each country, and the existing statistical methods have certain limitations. In economically developed countries and regions, official economic statistics can be regularly updated and published. Nevertheless, in some underdeveloped regions, especially in Africa, there are issues with the availability and quality of official economic statistics [14]. This issue has become a hot topic of current research; therefore, using multiple sources of spatial data to evaluate economic development levels has become a trending and prominent issue in the international research community. Utilizing multiple sources of spatial data can compensate for the limitations of traditional economic statistical data and provide a more comprehensive and accurate economic evaluation. This approach holds potential in addressing the issues of availability and quality of official statistical data, offering a more reliable foundation for policy formulation and decision-making. As a result, an increasing number of researchers are now focusing on and exploring the application of multiple sources of spatial data in economic development evaluation [15–20]. Their goal is to gain a better understanding and assessment of the true economic conditions.

In recent years, nighttime light data have been extensively utilized as spatial data for the evaluation of socio-economic development in geographical research [21–27]. Sutton and Costanza [28] made the first attempt in 2002 to spatially model global economic development using joint modeling and simulation of nighttime light intensity from DMSP/OLS nighttime light remote sensing images with GDP or industrial economic data. However, this type of data has a limitation known as the "saturation effect," where the maximum value of the grayscale is restricted to 63. As a result, regions with actual higher grayscale values can only be displayed as 63, and the spatial resolution of these data is relatively low. Since the emergence of the NPP-VIIRS nighttime light data in 2012, its high spatial resolution and accurate recording of nighttime light radiance have been widely applied. Wang [29] utilized NPP-VIIRS nighttime light remote sensing imagery to estimate and map the subnational GDP of Uganda based on an enhanced light intensity model. Li first proposed the application of nighttime light data to estimate the GDP of China in 2015 [30]. Li [31] conducted a another research on the spatiotemporal modeling of NPP-VIIRS nighttime light intensity and GDP in major urban agglomerations in China. The research aimed to validate the spatiotemporal heterogeneity of the proposed model. There have been numerous and rich research achievements in using NTL data for economic evaluation at different scales [32–34]. Despite the significant advantages of using nighttime light data in economic development evaluation, it is essential to recognize that nighttime light data can only capture artificial light during the night [17]. Moreover, nighttime light data can be influenced by various factors, including human activity intensity, observation angles, and abnormal noise [35]. Indeed, exploring other data sources is crucial to enhance the capabilities of economic evaluation. With the rapid development of technologies such as computers and the internet, spatial data collection has become more accessible. The concept of Volunteered Geographic Information (VGI) was first introduced by Goodchild [36] in 2007, and it refers to geographic data contributed voluntarily by the public [37]. OpenStreetMap (OSM) is considered one of the most prominent VGI projects [38]. OSM data

are globally available for free and is characterized by its rapid updates. In comparison to official statistical and commercial data that often require authorization or incur fees, and may have slower update rates [39], OSM data offer significant advantages, making them an invaluable data source. Indeed, OpenStreetMap (OSM) has evolved into an independent research field [40]. The characteristics of being massive, heterogeneous, rich, and freely available have drawn extensive attention from researchers to OpenStreetMap [41]. Research on OSM has primarily focused on OSM data quality assessment [40,42,43]. However, OSM research has expanded to various fields, including urban development [44–46], navigation, disaster relief, and humanitarian aid [47], among others. Although OSM data have been utilized in economic studies as well [48,49], the focus has mainly been on economically developed regions, and there is still a lack of research in economically underdeveloped areas. OSM data can be autonomously and freely uploaded by any individual or organization, and it is precisely this characteristic that establishes a strong correlation between the contribution of OSM data and the socio-economic conditions of the regions [50]. Scholars have applied OpenStreetMap (OSM) data and Nighttime Light (NTL) data in various geographical studies, encompassing climate, land use, and urban development. For example, Cheng utilized these datasets to discern alterations in urban land patterns across different developmental stages [51]. Shi employed OSM, NTL, and other data to categorize and identify local climate zones within specific regions, thereby contributing to a more accurate delineation of localized climatic patterns supporting large-scale production [52]. Wang employed both datasets to compute housing vacancy rates, successfully estimating these rates in cities with diverse developmental statuses [53]. Furthermore, Ma comprehensively examined the scaling attributes within urban areas by integrating OSM and NTL data, providing crucial data support for a nuanced understanding of urban planning and economic development [54]. This study aims to explore the capabilities of OSM data in economic development modeling, especially for economically underdeveloped areas. It employs the space-time geographically weighted regression method to investigate the combined modeling of OSM data and nighttime light data in assessing economic development. China's economic development exhibits significant spatial variations, with the eastern regions generally outperforming the western regions. Therefore, focusing on the Chinese mainland as the study area and assessing the differences in economic modeling using various spatial data in different regions will contribute to a better understanding of spatial data applications. This research will also serve as a reference for future studies in this field.

This study takes the Chinese mainland as an example to explore the capabilities of OSM data in economic development evaluation. It investigates the economic evaluation effects of OSM and NTL data when jointly modeling them in different regions. The structure of this paper is as follows: Firstly, an introduction to the research area, data selection, and methods used is provided. Secondly, the economic modeling effects of different spatial data are discussed. Based on the previous sections, the advantages and limitations of OSM, NTL, and their joint modeling at the prefecture-level city scale are discussed. Finally, the research results are summarized, and conclusions are drawn.

2. Data and Methods

2.1. Study Area

In order to assess the economic development evaluation modeling capabilities of OSM data and NTL data, this study focuses on four direct-controlled municipalities (Beijing, Shanghai, Tianjin, and Chongqing) and 332 prefecture-level cities (reduced to 331 after the 2019 merger of Jinan and Laiwu) and autonomous prefectures in the Chinese mainland (excluding Hong Kong, Macau, and Taiwan). The research area and the NTL data along with OSM Point of Interest (POI) and road network data for some cities are illustrated in Figure 1.

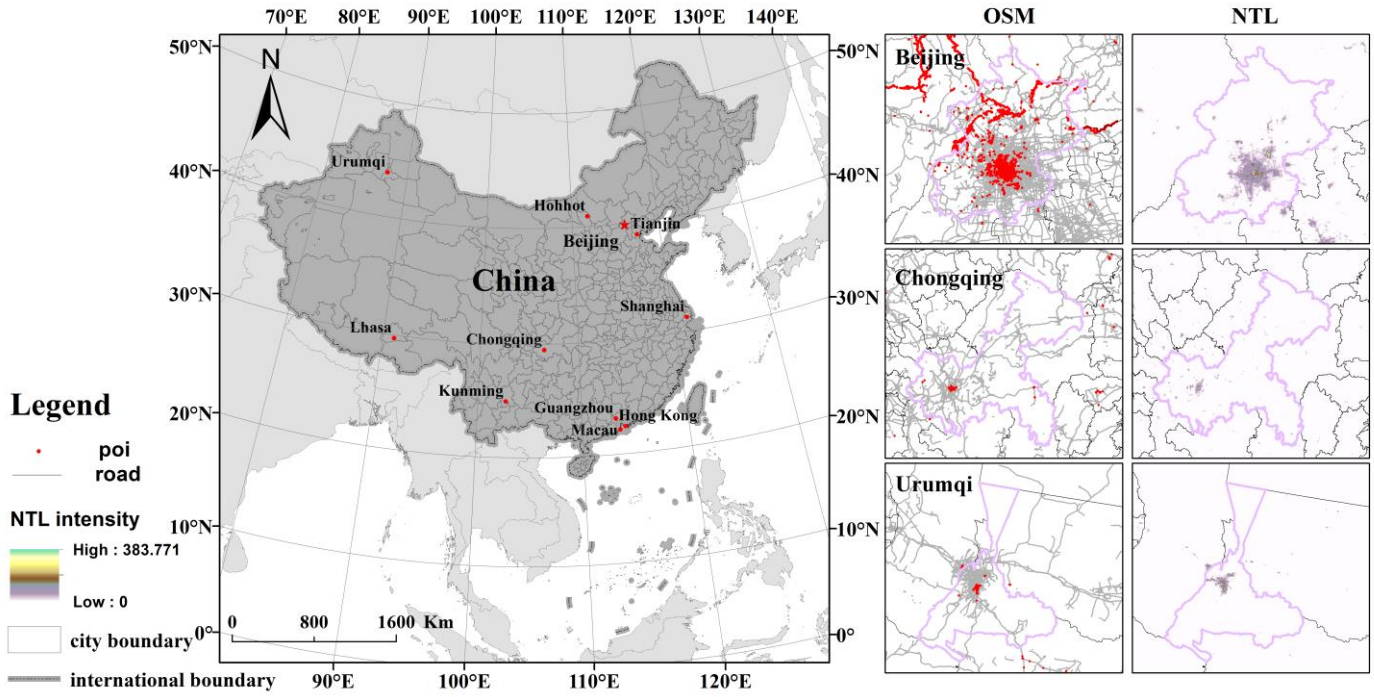

Figure 1. Research Area and NTL Data with OSM POI and Road Network Data for Some Cities.

2.2. Data

The research data includes OSM data, NTL data, and economic data from 2013 to 2021. We started from 2013 because OSM data, which are currently available for download, date back to that year. The variable descriptions and statistical data are presented in Table 1.

Table 1. Variable descriptions and statistics.

Data Name	Variable	Description	Unit	Min.	Max.	Standard Deviation
OSM	POI Count	POI Total Count	Per	0.00	14162	720.91
	POI Density	POI Density	Per/km^2	0.00	1.4690	0.08776
	Road Density	Road Network Density	km/km^2	0.0049	8.0836	0.76310
NTL	TNL	Total nighttime light		209.74	505,994	56,317.75
Economy	GDP	Gross Domestic Product	100 million CNY	7.3471	43,214.9	3846.57

The OSM data can be freely downloaded from the OSM website URL (download.geofabrik.de) in the ESRI Shapefile format. OSM data are open-access, allowing anyone to freely utilize, edit, and share this geographic information. OSM encompasses diverse geographical data, including road networks, points of interest (POI), topography, buildings, bodies of water, and more. The map data adhere to open standards, facilitating the import and export by various geographic information software and applications. The OSM data primarily include region POI count data, POI density data, and road network density data. POI data comprise specific points on a map, typically denoting locations of particular significance or attraction. POI categories encompass landmarks, dining establishments, accommodations, retail outlets, cultural and entertainment venues, recreational spaces, educational and research institutions, healthcare facilities, financial and service entities, public amenities, and corporate offices. These diverse POI categories span locations of potential interest to individuals in their daily lives and travels, serving as a comprehensive information foundation for the provision of personalized map services and navigation. The NTL data used in this study utilize the global 500-m resolution "NPP-VIIRS-like" nighttime light dataset [32] from URL (www.geodata.cn). This dataset possesses parameters and attributes consistent with NPP-VIIRS nighttime light data. Additionally, to obtain

a complete long time-series dataset spanning from 2000 to 2021, the annual composite NPP-VIIRS nighttime light data from 2013 to 2021 are appended directly to the existing "NPP-VIIRS-like" nighttime light data for the years 2000 to 2012.

2.3. Methods

2.3.1. Spatial Autocorrelation

Spatial autocorrelation measures the extent to which a particular geographic phenomenon or attribute value in one specific spatial unit correlates with the same phenomenon or attribute value in nearby spatial units [55]. To illustrate, if the values of a variable in one spatial unit closely resemble those in its neighboring units, consistently being either high or low, it indicates a positive spatial autocorrelation. Conversely, if the values significantly differ, it implies a negative spatial autocorrelation. This study employs GeoDa [56] for spatial autocorrelation analysis. Given the irregularities in administrative boundaries, the utilization of the queen contiguity matrix is deemed a practical approach, especially suited for handling polygonal regions. Specifically, the study used queen adjacency to construct the spatial weight matrix, with an adjacency rank of 1.

(1) Global spatial autocorrelation

Global spatial autocorrelation pertains to the overall spatial clustering characteristics within a given region [57,58]. Moran's I [59] serves as a vital metric for quantifying global spatial autocorrelation. Moran's I ranges from -1 to 1, where a value exceeding 0 signifies positive spatial correlation and a tendency toward spatial clustering of the variable in question. Conversely, a value below 0 suggests negative spatial correlation and a tendency toward spatial dispersion of the variable. Through an analysis of global autocorrelation, we can discern spatial clustering patterns within the OSM data.

(2) Local spatial autocorrelation

Local spatial autocorrelation [60] primarily explores the specific characteristics of spatial clustering within an area. Unlike the global Moran's test, local spatial autocorrelation overcomes the limitation of ignoring local spatial clustering [61,62].

According to the calculation results, the clustering states can be divided into high-high aggregation (H-H), low-low aggregation (L-L), high-low aggregation (H-L), and low-high aggregation (L-H). The spatial clustering distribution characteristics of OSM data can be observed through local spatial autocorrelation.

2.3.2. Geographically and Temporally Weighted Regression Model

The GTWR model is an extension of the Geographically Weighted Regression (GWR) model and is a local regression model that considers spatial and temporal variations [63–65]. It utilizes regional panel data for spatial regression and links the time attribute to the spatial attribute of geographically weighted regression, better reflecting the spatiotemporal information of the regions and improving the efficiency of estimation [66]. By analyzing the regression results of the GTWR model, one can make more effective judgments about the spatial heterogeneity of spatial data in economic development evaluation. The expression of the GTWR model is as follows [65]:

$$y_i = \beta_0(u_i, v_i, t_i) + \sum_{k=1}^{p} \beta_k(u_i, v_i, t_i) X_{ik} + \varepsilon_i,\ i = 1,\ 2,\ \ldots,\ n \tag{1}$$

where, (u_i, v_i, t_i) is the space-time coordinate of point i, u_i, v_i, t_i, respectively, represent the longitude, latitude, and time of point i, $\beta_0(u_i, v_i, t_i)$ is the constant term, $\beta_k(u_i, v_i, t_i)$ represents the k-th regression coefficient of point i, and ε_i is the model residual term.

The point i regression coefficient β_i can be calculated by the least square method:

$$\beta_i(u_i, v_i, t_i) = \left(X'W(u_i, v_i, t_i)X\right)^{-1} X'W(u_i, v_i, t_i)y_i \tag{2}$$

In the equation, $W(u_i, v_i, t_i)$ represents the spatiotemporal weight matrix, which uses a Gaussian function as the weight function. The selection of bandwidth significantly influences the establishment of spatiotemporal weights. This study utilizes the AICc method for adaptive bandwidth determination, with the numerical value of the bandwidth indicating the number of neighboring cities.

2.3.3. Residual Analysis

Residual analysis is a common statistical method used to evaluate how well a regression model fits the data and to understand the properties of the model's errors. Residuals represent the differences between the predicted values and the actual observed values of the dependent variable when using the model for predictions. This analysis is essential for assessing the accuracy of regression results, especially in the context of spatial data. Absolute and relative residuals can be calculated as follows:

$$R_{Absolute} = Predictive_i - Real_i \; i \in [1, 2, 3, \ldots, 3021] \tag{3}$$

$$R_{relative} = \frac{(Predictive_i - Real_i)}{Real_i} \times 100\% \; i \in [1, 2, 3, \ldots, 3021] \tag{4}$$

where i is each prefecture-level city from 2013 to 2021, $Predictive_i$ is the model forecast GDP, and $Real_i$ is the real GDP.

2.3.4. Regression Model Parameters and Description

Adjusted R^2 is a metric used to measure the goodness of fit for a linear regression model. In comparison to the ordinary R^2, it accounts for model complexity by adjusting for degrees of freedom, providing a more reliable reflection of the model's explanatory power on real data.

AICc [67] (Akaike Information Criterion with correction) serves as an indicator for comparing statistical models, taking into consideration both the goodness of fit and model complexity. Particularly suitable for small sample sizes, a smaller AICc value indicates a more optimal model.

3. Results

3.1. Analysis of OSM Features and Modeling Capability

3.1.1. Residual Analysis

Figure 2 and Table 2 depict China's global Moran's Index for OSM data. Notably, the Moran's Index of OSM data remains consistently positive from 2013 to 2021. Among the three variables, road network density displays the highest Moran's Index, outperforming POI count and POI density.

Over the years, the Moran's Index of POI count decreases, while POI density experiences a slight increase. Conversely, road network density's Moran's Index exhibits an upward trend, signaling a spatial clustering pattern within China's OSM data. Furthermore, clustering in POI count and density is waning, whereas road network density's clustering is strengthening. These trends were statistically confirmed, with all p-values below 0.05.

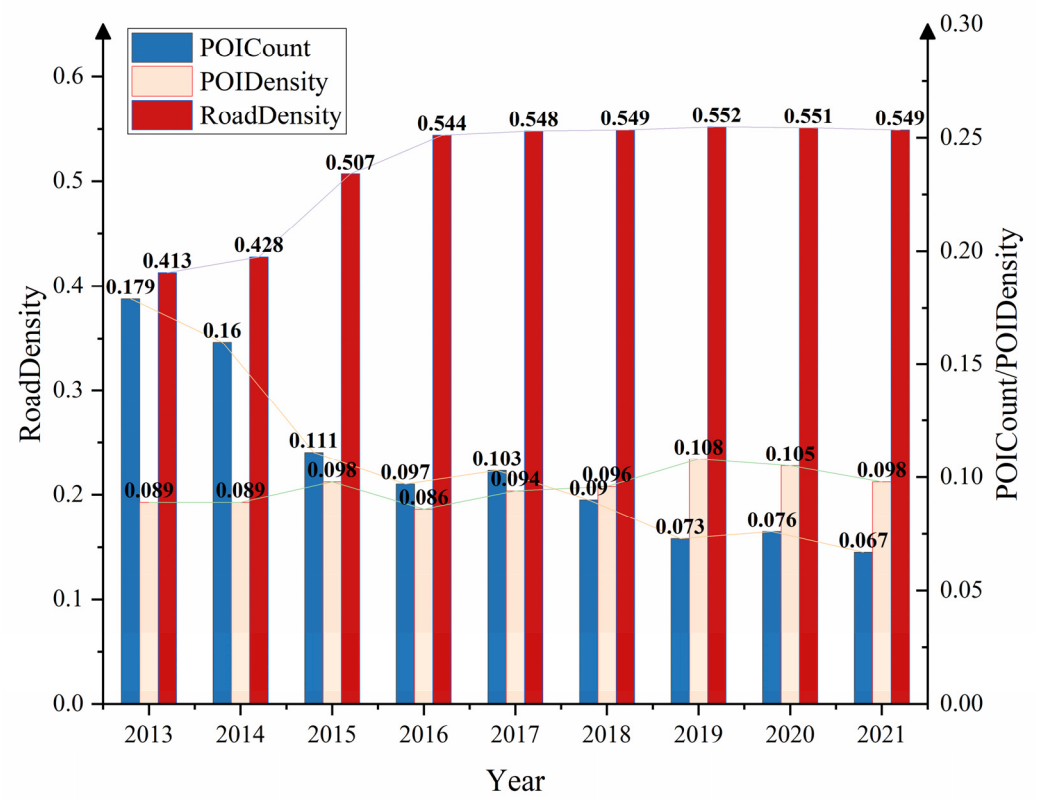

Figure 2. Variation chart of Moran's Index of OSM data from 2013 to 2021.

Table 2. Variable descriptions and statistics on the Moran Index.

Data	Year	Moran Index	*p*-Value	Z-Value
POI Count	2013	0.179	0.002	6.564
	2014	0.16	0.003	5.909
	2015	0.111	0.011	3.676
	2016	0.097	0.014	3.562
	2017	0.103	0.015	3.537
	2018	0.09	0.016	3.511
	2019	0.073	0.029	2.46
	2020	0.076	0.026	2.529
	2021	0.067	0.032	2.285
POI Density	2013	0.089	0.017	2.931
	2014	0.089	0.013	3.091
	2015	0.098	0.005	3.478
	2016	0.086	0.018	2.849
	2017	0.094	0.017	2.969
	2018	0.096	0.018	3.099
	2019	0.108	0.009	3.582
	2020	0.105	0.011	3.405
	2021	0.098	0.011	3.203
Road Density	2013	0.413	0.001	12.549
	2014	0.428	0.001	13.49
	2015	0.507	0.001	14.785
	2016	0.544	0.001	16.019
	2017	0.548	0.001	16.717
	2018	0.549	0.001	16.28
	2019	0.552	0.001	16.299
	2020	0.551	0.001	16.192
	2021	0.549	0.001	16.034

3.1.2. Local Spatial Autocorrelation Features

To delve into the local spatial characteristics of OSM data from 2013 to 2021, spatial autocorrelation analysis was performed. This analysis unveiled significant disparities between eastern and western regions, highlighted by the Hu Line [68], an east-west economic demarcation. Separating the region based on this line offers insights into economic differences and aids in explaining spatial autocorrelation.

The OSM local spatial autocorrelation map (Figures 3–5) reveals that H-H regions are predominantly found in economically developed areas like Beijing, Shanghai, and Guangzhou, while L-L regions are concentrated west of the Hu Line. The spatial local autocorrelation results all passed the significance test with p-values less than 0.05. This spatial pattern correlates with economic development levels, providing essential preliminary information for subsequent modeling.

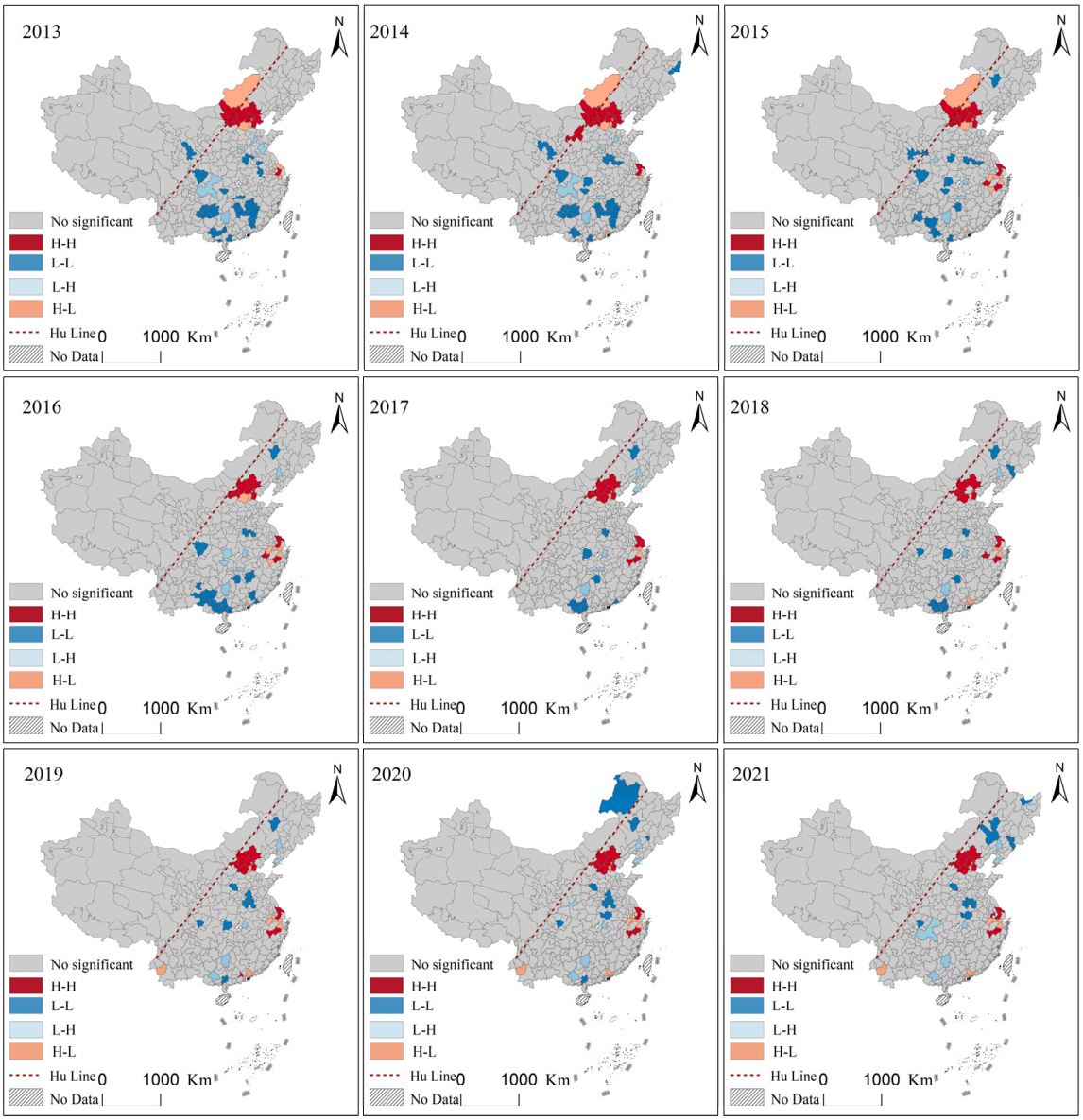

Figure 3. Local autocorrelation distribution of OSM POI count data from 2013 to 2021.

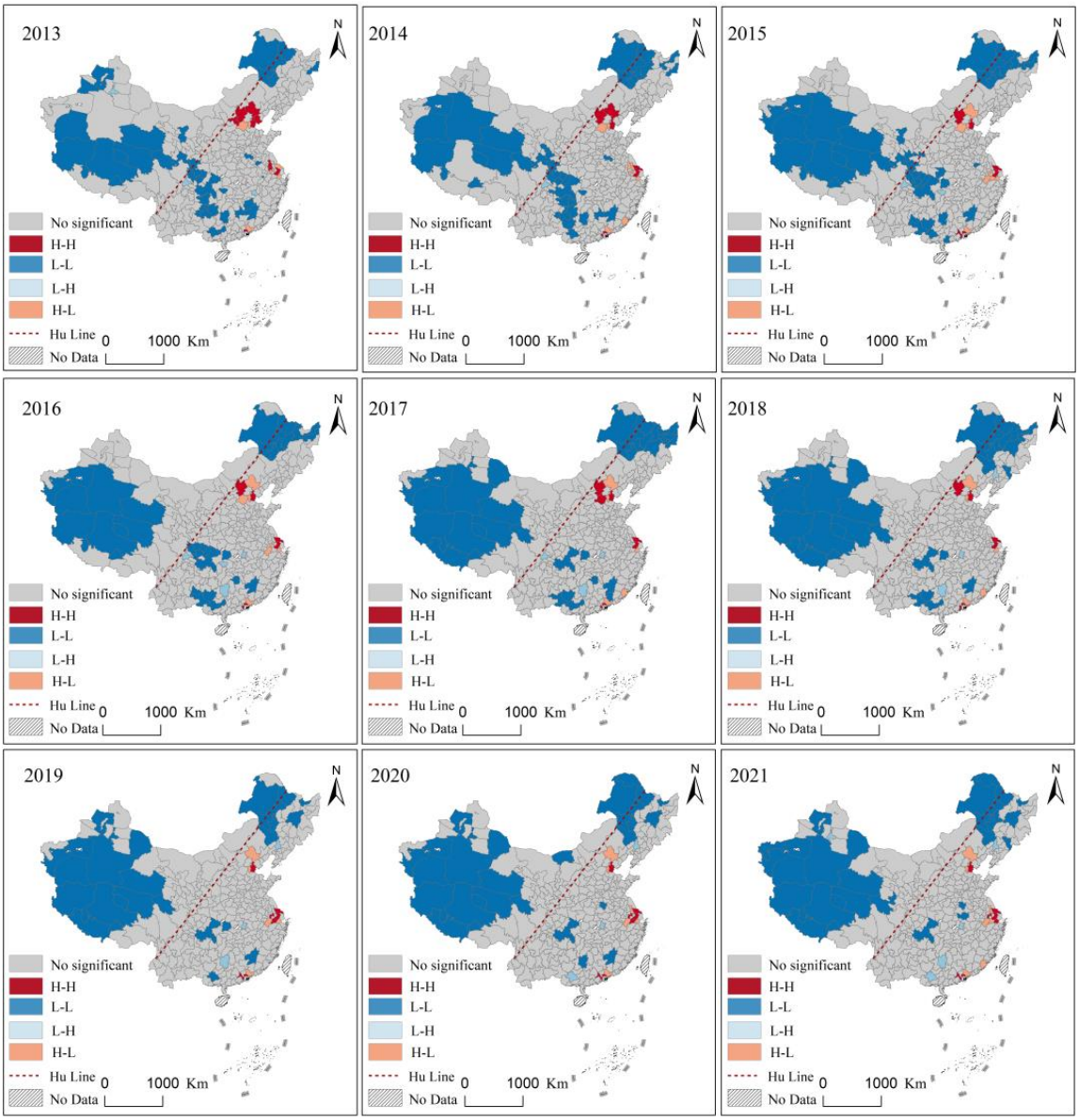

Figure 4. Local autocorrelation distribution of OSM POI density data from 2013 to 2021.

3.1.3. Analysis of OSM Economic Modeling Capability

To explore the economic modeling capability of spatial data, we first conducted regression analyses using OLS, GWR, and GTWR on the OSM data. GDP was chosen as the dependent variable. To achieve better results with fewer variables and avoid multicollinearity issues during analysis, we conducted exploratory analysis in ArcGIS to select indicators with significance greater than 50% and Variance Inflation Factors (VIF) less than 7.5. The VIF for the selected variables in this study are as follows: POI count = 3.37, POI density = 3.48, road network density = 2.97, the total nighttime light = 3.01. As a result, we selected POI count, POI density, and road network density as explanatory variables for the economic modeling. The annual regression results are summarized in Figure 6. The comparison between GTWR regression results and OLS results for the years 2013–2021 is shown in Table 3.

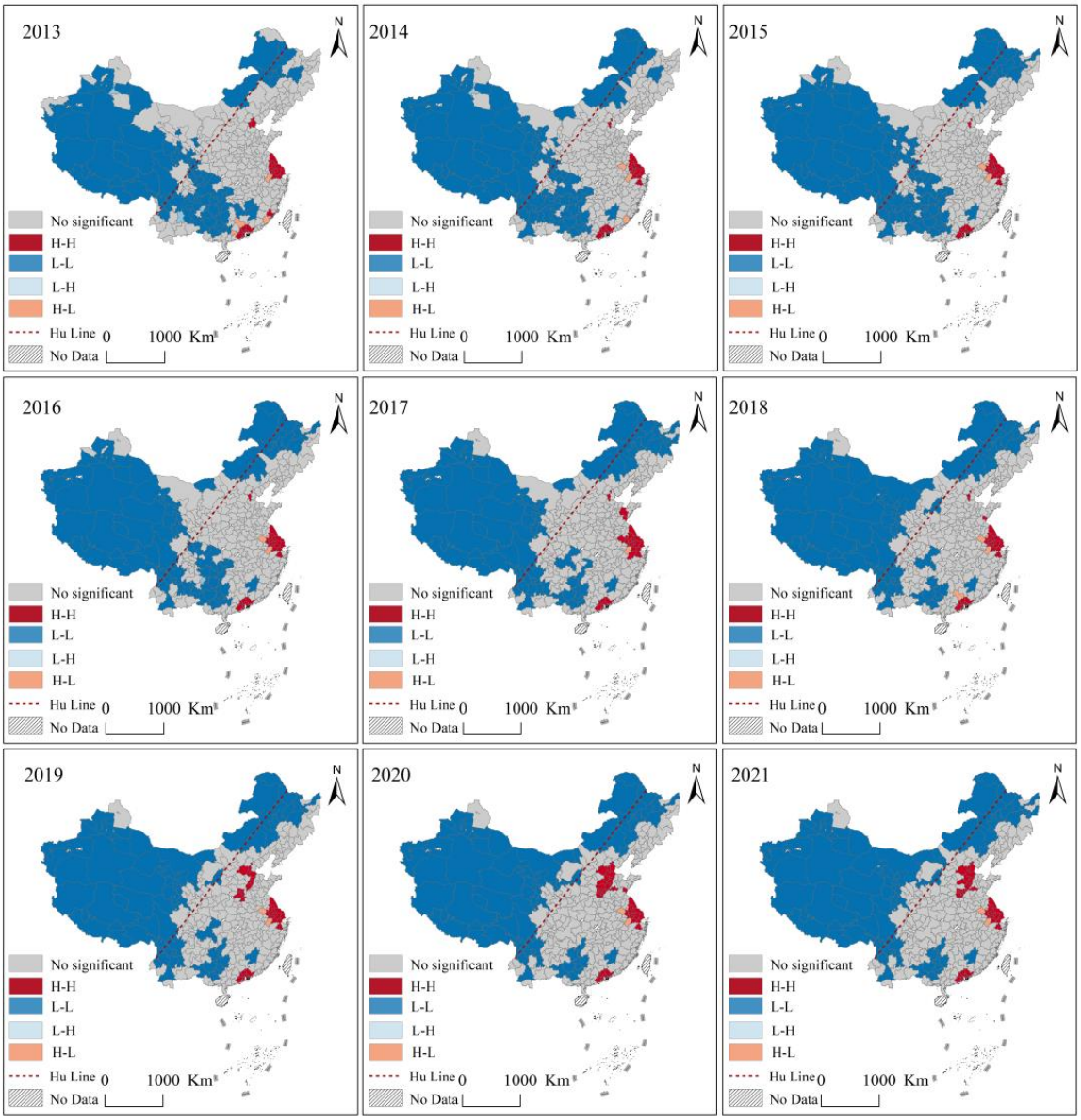

Figure 5. Local autocorrelation distribution of OSM road density data from 2013 to 2021.

Table 3. OLS and GTWR modeling results of OSM data.

Model	R^2	Adjusted R^2	AICc	Bandwidth
GTWR	0.898	0.889	51,992.28	16
OLS	0.675	0.674	55,066.95	

Figure 6 illustrates that the GWR results surpass OLS, with a noteworthy improvement of 0.214 in adjusted R^2 and a substantial decrease of 3074.68 in AICc [67] (in model comparisons using AICc, a difference greater than 3 indicates the model with the lower AICc is the better fit [69–71]). Furthermore, the economic modeling with OSM data has shown consistent enhancement, with adjusted R^2 rising from 0.717 in 2013 to 0.844 in 2021. Additionally, local R^2 values are presented in Figure 7.

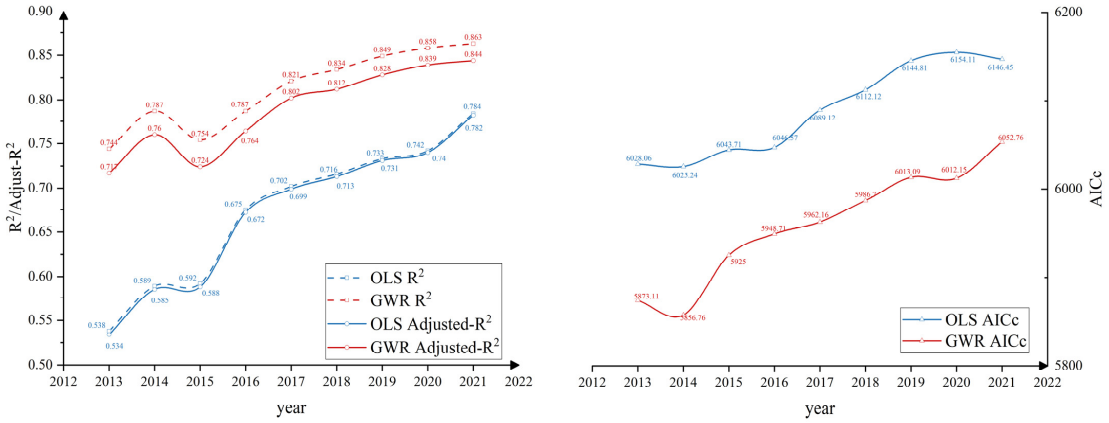

Figure 6. OLS and GWR modeling results of OSM data.

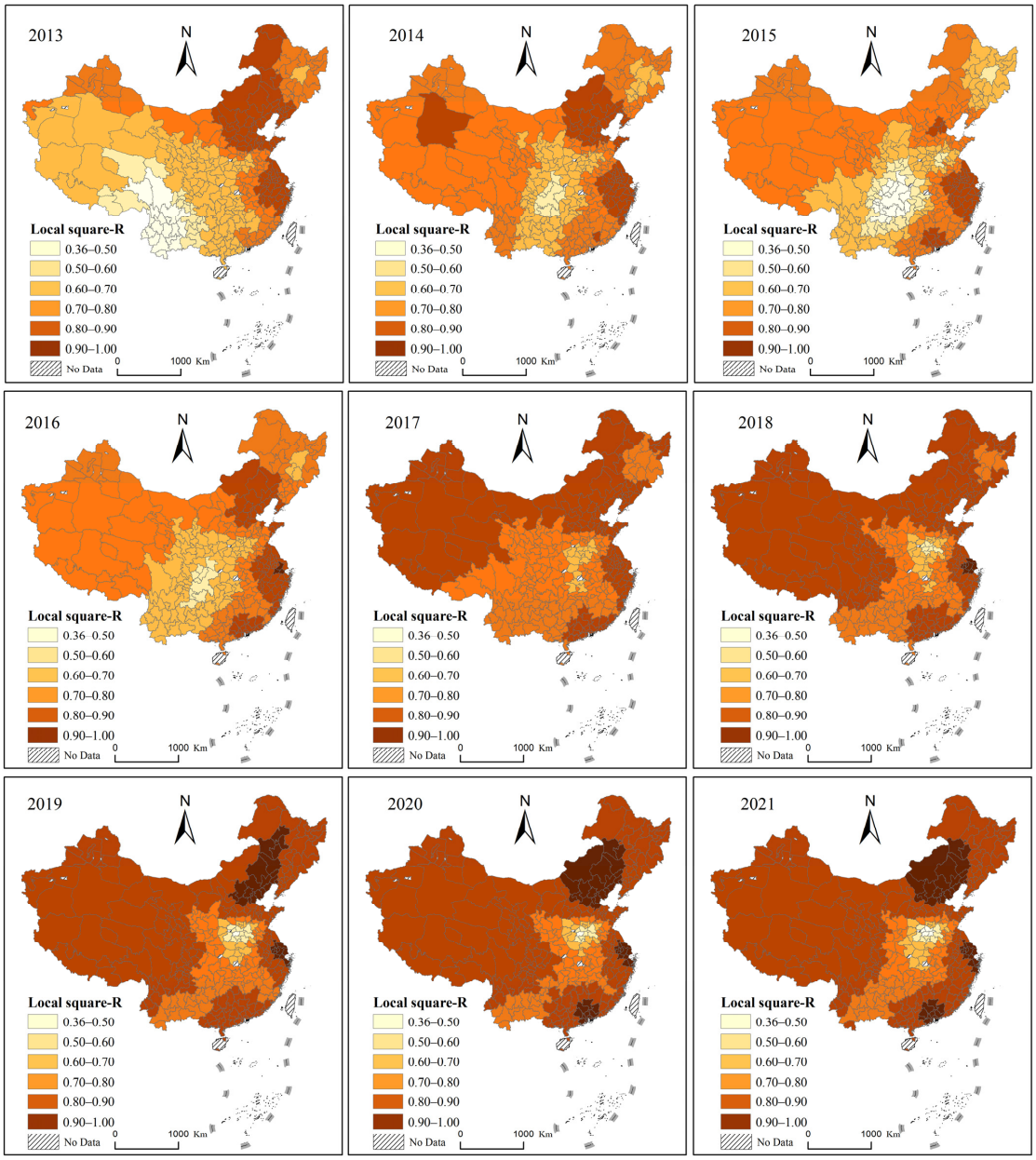

Figure 7. OSM data local R^2 of the GWR model for each year.

3.2. Analysis of NTL Economic Modeling Capability

As a data parameter widely used in economic evaluation [31,33], NTL was analyzed using the same model as OSM to compare the differences in their effectiveness in evaluating the economy. The annual regression results of NTL are summarized in Figure 8 and the comparison results between GTWR and OLS for the years 2013–2021 can be found in Table 4. Additionally, local R^2 values are presented in Figure 9.

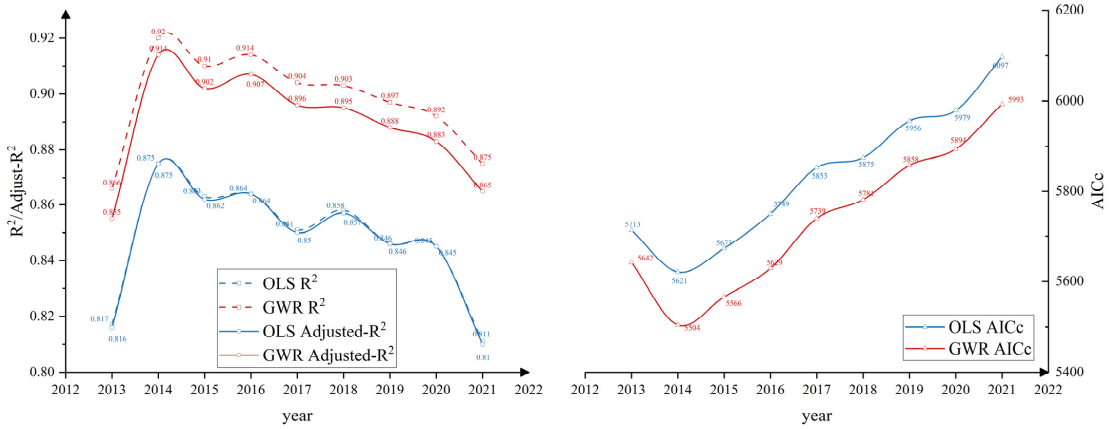

Figure 8. OLS and GWR modeling results of NTL data.

Table 4. OLS and GTWR modeling results of NTL data.

Model	R^2	Adjusted R^2	AICc	Bandwidth
GTWR	0.915	0.911	51,200.73	26
OLS	0.842	0.842	52,882.25	

From Figure 8, it is evident that NTL's GWR results outperform OLS, reflected in the improved adjusted R^2 and reduced AICc. Additionally, NTL excels over OSM in GDP modeling, offering a better fit. However, NTL's fitting performance gradually declines from 2014 to 2021, reaching an adjusted R^2 of 0.865 in 2021. Conversely, OSM's 2021 adjusted R^2 is 0.844, indicating a rising trend and an approach to NTL's economic modeling capabilities.

As shown in Table 4, the GTWR modeling results using NTL are significantly better than OLS, with an increase in adjusted R^2 of 0.069 and a decrease in AICc of 1681.25. This indicates that the GTWR model exhibits a substantial advantage in economic modeling compared to OLS.

From Figure 9, in 2013, NTL modeling had low performance near the Hengduan Mountains in southwest China. Between 2014 and 2017, NTL exhibited strong fitting performance nationwide, with local $R^2 > 0.8$. It excelled in eastern coastal areas, the northeast, and southwestern China, with local $R^2 > 0.9$. However, starting in 2018, NTL's performance weakened in the Pearl River Delta region. By 2021, there was a significant decline in NTL's fitting performance, especially in southern China, where it was notably poor.

3.3. Joint Modeling Results of OSM and NTL

In the previous section, we assessed OSM and NTL data's individual economic modeling capabilities. Now, we aim to combine these datasets as independent variables to jointly model GDP, exploring the potential of multi-sourced spatial data for economic modeling.

The results of the joint modeling with OSM and NTL data are presented in Table 5. We employed both GTWR and OLS models for modeling, ensuring that all independent variables had VIF values below 7.5. As shown in the table, GTWR modeling significantly outperforms OLS modeling, with an adjusted R^2 of 0.957 for the GTWR model, surpassing the adjusted R^2 values of 0.911 for the NTL model and 0.889 for the OSM model. Moreover, the AICc value of the GTWR model is 2750.94, lower than that of the OLS model.

Furthermore, the joint modeling results using both OSM and NTL data exhibit a distinct advantage over single spatial data modeling. The combined GTWR model attains the highest adjusted R^2 value, indicating a superior fit to the data and a more accurate representation of economic relationships through the combined use of OSM and NTL data.

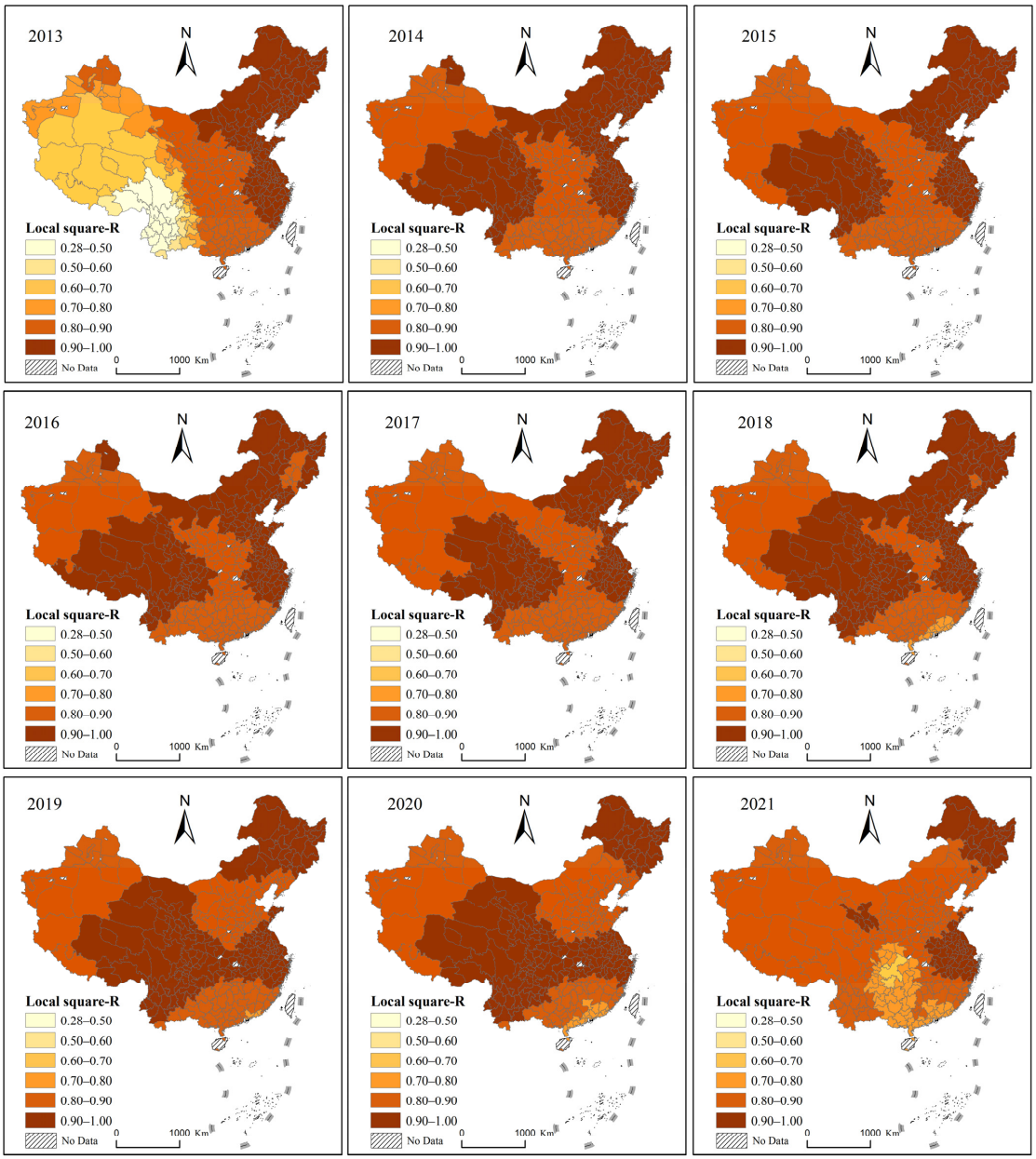

Figure 9. NTL data local R^2 of GWR models per year.

Table 5. Modeling results of OLS and GTWR combined with OSM and NTL.

Model	R^2	Adjusted R^2	AICc	Bandwidth
GTWR	0.960	0.957	49,112.71	26
OLS	0.887	0.887	51,863.65	

From Table 6, we observe that from 2013 to 2021, 90.04% of the 3021 analyzed prefecture-level cities had a local R^2 exceeding 0.9, while 9.04% had local R^2 values from 0.8 to 0.9. Only 0.93% had local R^2 values less than 0.8. In 2021, Chongqing had a local R^2 of 0.799, being the sole city with a value between 0.7 and 0.8. Cities with local R^2 below

0.7 were all in Yunnan Province. Diqing Tibetan Autonomous Prefecture had the lowest local R^2 of 0.412 in 2021, the lowest nationwide. From 2013 to 2020, its local R^2 ranged from 0.474 to 0.659. Two other cities with relatively lower local R^2 values were Nujiang Lisu Autonomous Prefecture (2021: local R^2 0.543; 2013–2020: local R^2 0.592) and Lijiang (2021: local R^2 0.613; 2013–2020: local R^2 0.659).

Table 6. OSM and NTL joint modeling R^2 statistics.

Local R^2	Number of Cities	Percentage (%)
0.4–0.5	9	0.30
0.5–0.6	9	0.30
0.6–0.7	9	0.30
0.7–0.8	1	0.03
0.8–0.9	273	9.04
0.9–1.0	2720	90.04

Due to the consistent local R^2 values of GTWR across 2013–2020 (rounded to three decimal places), this study presents local R^2 values for 2013 and 2021, shown in Figure 10. It reveals that the joint modeling of OSM and NTL data fits well in economically developed regions in eastern China and economically underdeveloped regions. However, the fit is comparatively lower in regions with complex terrain and significant topographic variations. For example, Chongqing, often referred to as a "mountain city", and areas like Diqing Tibetan Autonomous Prefecture, Nujiang Lisu Autonomous Prefecture, and Lijiang, located in the mountainous Hengduan region, show less fitting due to their rugged topography. In summary, utilizing multiple spatial data for economic evaluation is feasible, yielding an excellent fit in most regions and still offering a good fit in economically underdeveloped areas.

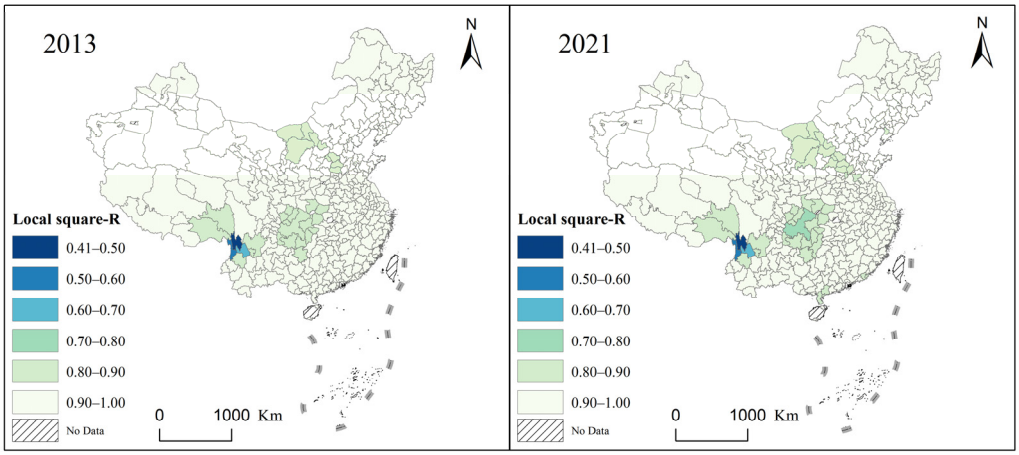

Figure 10. Local R^2 of the association between OSM and NTL.

To validate the regression model utilizing OSM and NTL data from 2013 to 2021, this study conducted residual analysis. Figures 11 and 12 present absolute residual scatter plots and spatial distribution maps, while Figures 13 and 14 show relative residual scatter plots and distribution maps.

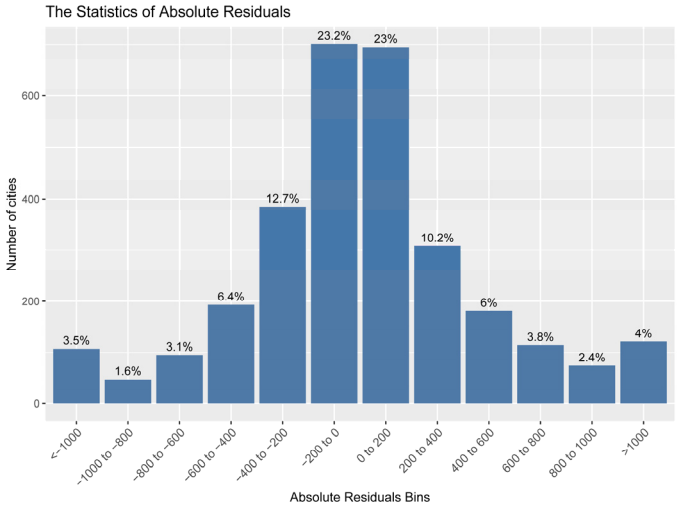

Figure 11. Statistical graph of absolute residuals of OSM and NTL combined.

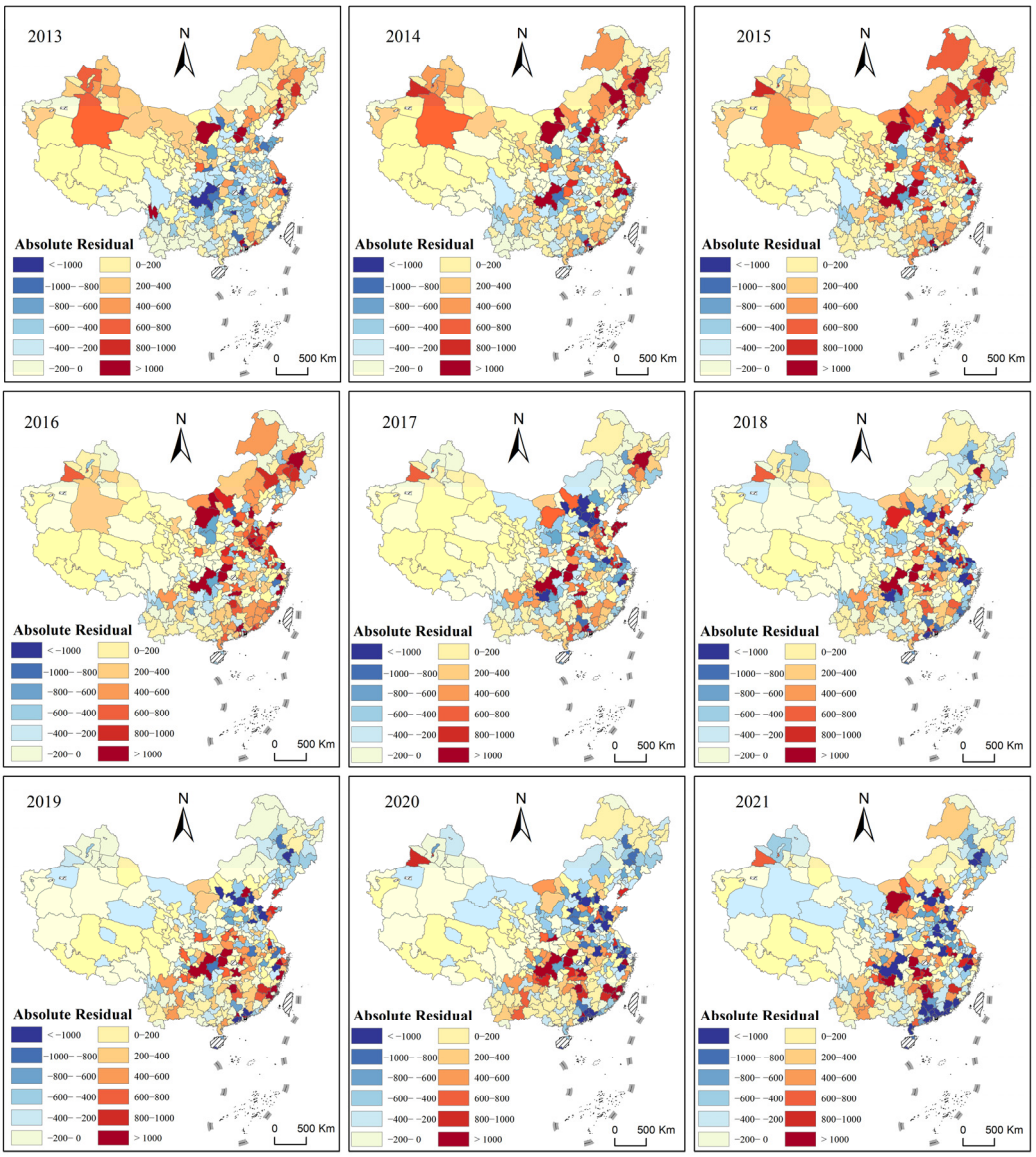

Figure 12. Distribution of absolute residuals of OSM and NTL combined.

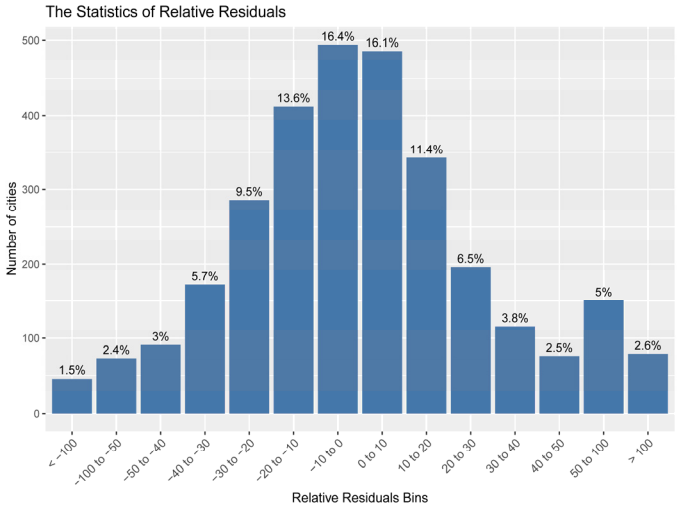

Figure 13. Statistical diagram of relative residuals of OSM and NTL combined.

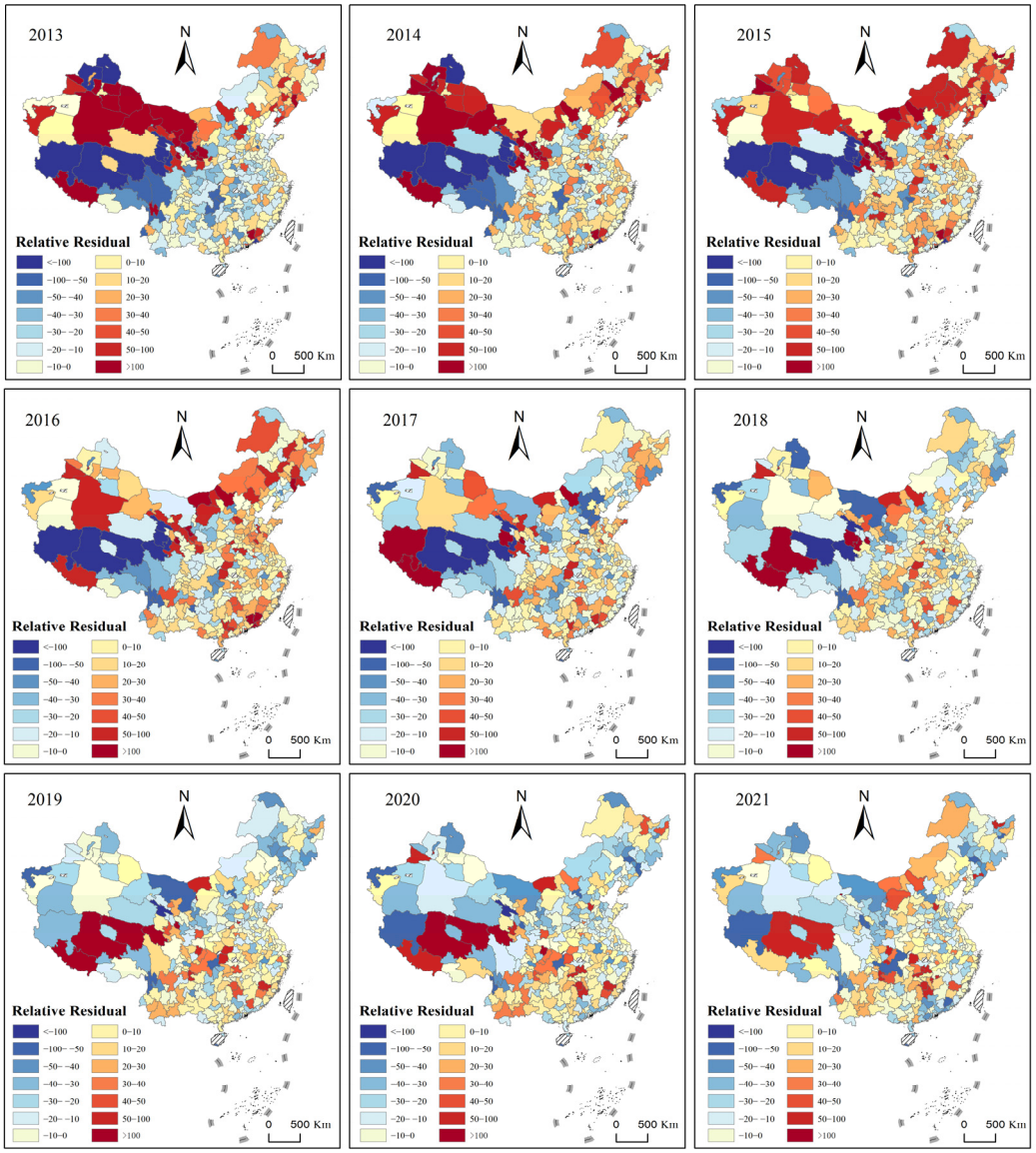

Figure 14. Relative residual distribution of OSM and NTL combined.

Figure 11 reveals that absolute residuals exhibit a normal distribution. Across all prefecture-level cities during this period, 46.2% have absolute residuals within the range of −200 billion to 200 billion yuan. Meanwhile, 7.5% exhibit extreme values exceeding 1000 billion yuan or falling below −1000 billion yuan. Notably, economically developed cities like Chongqing, Guangdong, Hubei, Hebei, and Zhejiang show substantial absolute residuals, while their relative residuals remain moderate (as depicted in Figure 13). Figure 13 indicates that relative residuals also follow a normal distribution. Among all prefecture-level cities, 32.5% have relative residuals within −10 to 10, 57.5% within −20 to 20, and only 4.1% with extreme relative residuals surpassing 100 or falling below −100. The latter are primarily concentrated in underdeveloped regions of western China, including Xinjiang, Qinghai, Tibet, Gansu, and Yunnan. However, their absolute residuals are not high.

4. Discussion

4.1. Economic Modeling Capabilities of OSM

The ability of OSM data as an economic evaluation indicator has been steadily increasing over the years, and GTWR can serve as an economic development evaluation model. The research findings indicate that the fit of OSM data to GDP shows a progressively improving trend (Figure 6). The reason why OSM has a good economic evaluation ability is mainly due to scholars' discoveries through various statistical analyses that there is a correlation between OSM contributions and the socio-economic characteristics of regions [50,72–74]. Unlike OSM data, NTL data have shown a declining trend in fit since 2014. During 2020–2021, there was a noticeable decrease in the fit between NTL and the economy, which could be attributed to the following factors. Firstly, POIs usually represent (urban) functional developments, and NTL data may represent morphological expansion in both space and quality [75–77]. Secondly, stringent lockdown measures were implemented in the Chinese mainland during the COVID-19 pandemic. Thirdly, this might be associated with the real estate bubble in the Chinese mainland. These factors could have contributed to a disparity between nighttime light intensity and economic development. Moreover, the model selected in this study has a higher fitting performance for GDP. Compared with the OLS model, the GTWR model can better study the heterogeneity of GDP in time and space scales. In comparison to other studies on economic development evaluation, this study demonstrates competitive performance with respect to the selected data sources and methods. For instance, Yu conducted regression analysis using corrected NPP-VIIRS data and GDP at the municipal level, achieving an R^2 value of 0.8088 [34]. Li investigated the correlation between per capita luminosity and per capita GDP in five Central Asian countries, but the R^2 values were not higher than 0.6 [78]. Another study by Li focused on China's mainland and found R^2 values of 0.8699 and 0.8544 between NPP-VIIRS TNL and GDP at the provincial and county levels, respectively [25]. Liu utilized OSM's road network density for regression analysis in 85 cities in China's provincial capitals and more developed eastern regions [48]. However, they did not study cities in less developed regions of the country and did not provide the overall R^2. Furthermore, Huang et al. utilized location-based social media (LBSM) data and NTL data with the GWR model to estimate the economic development potential at different scales in China [79]. Their regression analysis at the municipal level showed R^2 values of 0.846 for NTL and 0.827 for Tencent user density (TUD), which were lower than the R^2 values achieved in this study. The study uses OSM data (POI and road network) and NTL data (TNL) through the GTWR model for regression analysis at the municipal level. Compared with previous research, the study demonstrates good performance not only in economically developed areas but also in economically less developed regions, allowing for economic development evaluation in areas with limited economic data. Although the current economic evaluation capability of OSM data is slightly lower than that of NTL data, OSM's evaluation capability is increasing annually, and its faster and more convenient processing suggests that it may become a data source with superior economic evaluation performance in the near future. This highlights

the importance of continuously exploring and advancing the use of spatial data sources for economic development assessment.

4.2. Multi-Source Data Evaluation of Economy

Using multiple data sources for economic evaluation provides a more comprehensive, accurate, and reliable assessment, while relying on any single data source for economic evaluation is not sufficiently objective and comprehensive. Official GDP statistics are the most widely used economic evaluation panel data [3], but the reliability of official GDP data may be questionable in some low-income or middle-income countries [63]. Due to its high spatial and temporal resolution and consistent global coverage, NTL data have become an alternative to GDP for measuring regional economic development using spatial data. However, the accuracy of NTL data can be affected by human activities and other sources of abnormal light [66]. Currently, NTL data still show a high level of fitting performance for economic evaluation. Nevertheless, this study observed a gradual weakening of the fitting performance of NTL for economic evaluation after 2014 (Figure 8). Inspired by the use of multi-source data in remote sensing, this study suggests that using multi-source data to evaluate economic development may lead to better results. Evaluating economic development with multiple data sources not only compensates for the limitations of using a single indicator (such as unreliable GDP data or potential falsification) but also offers a more efficient and cost-effective approach compared to conventional panel data used for economic evaluation. Moreover, multi-source spatial data for economic evaluation are not constrained by administrative boundaries, making it a valuable tool for regional spatial planning, development, and governance, providing better support for decision-making. As shown in Table 5, this study utilized four indicators from two spatial data sources for economic development modeling, achieving an adjusted R^2 of 0.957, which outperforms any single indicator in evaluating economic development. In comparison, Cui used a comprehensive nightlight composite economic index constructed from NTL data, Normalized Difference Vegetation Index (NDVI) data, POI data, and urban land use data for economic modeling, obtaining a correlation with the total social retail sales of consumer goods with an adjusted R^2 of 0.76 [80]. The use of spatial data for economic evaluation not only offers faster and more flexible data acquisition compared to traditional statistical data but also allows customization of regions based on specific user needs, without being constrained by administrative boundaries. As an important source of geographical big data, Volunteered Geographic Information (VGI) data can provide a wealth of information for economic evaluation. In addition to the classical OSM data selected in this study, Wikimapia, Google Map Maker, and various location-based social applications such as Tencent, Weibo, Facebook, and Twitter can all serve as valuable data sources for economic evaluation. The integration of multiple spatial data sources allows for more precise economic evaluation. However, in the context of using multiple spatial data sources for economic evaluation, the consideration of massive data application may lead to challenges related to time and cost. In such research, it is crucial to first conduct exploratory analysis on similar data types and then select appropriate VGI data sources tailored to the specific study area and available hardware facilities, adhering to the principle of situational appropriateness.

4.3. Limitations and Prospects

Leveraging the GTWR model for joint economic modeling of OSM and NTL data yields strong overall performance. This integration of multisource spatial data enhances the model's capacity to capture spatiotemporal variations and economic development correlations, providing a more accurate and comprehensive economic assessment. Nonetheless, it is worth noting that in regions characterized by rugged terrain and limited infrastructure, where economic development relies predominantly on nature and cultural tourism, the spatial data might not fully reflect the true economic development levels, leading to potential underestimations.

This study focused solely on prefectural-level analysis, excluding provincial or county levels. Additionally, we did not cross administrative boundaries for simulations due to our use of GDP data based on administrative divisions. We have demonstrated the potential of prefectural-level analysis using various spatial data sources, but have not explored cross-scale model performance in this research. Future research endeavors should take into account spatial scale effects [81] by employing multi-scale data analysis and model evaluation. To delve deeper, the exploration should transcend administrative boundaries, focusing on grid-scale dynamics and the perspectives offered by natural cities [82,83]. This nuanced approach aims to enhance comprehension of economic development, thereby delivering more precise and targeted recommendations for decision-makers.

While China's regions can represent areas with different levels of economic development, the applicability of using multiple spatial data sources for economic evaluation on a global scale still needs to be further investigated. Based on the aforementioned limitations, future research will attempt to explore the capabilities of using multiple spatial data sources to evaluate economic development at different scales and in different regions. By integrating and analyzing various data sources, we can achieve a more comprehensive and accurate assessment of economic development. This comprehensive analysis of multiple data sources is expected to provide deeper insights and reveal the heterogeneity of economic development across different regions and scales. This will offer a more reliable and comprehensive evaluation method for regional quantitative economic studies and provide stronger support for the formulation of effective development policies.

5. Conclusions

This study focused on Chinese mainland prefectural-level cities, and explored the modeling potential of OSM data and their combination with NTL data for economic development analysis. The comprehensive utilization of multiple spatial data sources provides a more accurate and comprehensive analytical framework for economic development evaluation. Our approach can overcome the limitations of traditional single data sources and offer decision-makers a more precise tool for economic development assessment. Furthermore, the application of multiple spatial data sources can provide strong support for the economic development of developing countries and serve as a decision-making reference for achieving SDG-10 (reducing inequality). These research findings hold significant practical significance, enabling policymakers to better understand and promote economic development, thereby fostering social inclusivity and sustainable development. The main conclusions are as follows:

(1) The GTWR model was used to evaluate economic development with OSM data as the single data source from 2013 to 2021, resulting in an R^2 of 0.898 and an adjusted R^2 of 0.889. When NTL was used as the single data source for economic development evaluation, the R^2 was 0.915, and the adjusted R^2 was 0.911. OSM data can be considered as a metric to assess economic development, and its evaluation effectiveness is steadily increasing over the years. On the other hand, the evaluation effectiveness of NTL data, as a conventional spatial metric for economic development, is declining. OSM data demonstrate strong correlation with regional socio-economic factors and offer significant advantages over commercial and official maps for economic development evaluation.

(2) The integration and fusion of multiple spatial datasets can serve as a measurement data source for evaluating the spatiotemporal development characteristics of regional economies. The evaluation of economic development using multiple spatial data sources is more reliable than relying on a single data source. VGI data like OSM and spatial metrics like NTL offer empirical and applied research examples for evaluating regional economic development in China. They provide support for broader research and applications in this field.

(3) The GTWR model takes into account spatial and temporal heterogeneity, allowing the establishment of separate regression models at different spatial and temporal points.

This enables a more accurate capture of spatiotemporal variations in regional economic characteristics. Compared to conventional global regression analysis, GTWR offers better accuracy and explanatory power in spatiotemporal evaluation of regional economies, resulting in more accurate and reliable assessments of economic development.

Author Contributions: Methodology, Z.W., J.Z., C.H. and B.L.; Software, Z.W. and B.L.; Resources, J.Z.; Data curation, Z.W.; Writing—original draft, Z.W.; Writing—review and editing, J.Z., C.H., B.L., D.Y., J.Y. and L.H.; Supervision, J.Z.; Funding acquisition, J.Z. All authors have read and agreed to the published version of the manuscript.

Funding: The Third Comprehensive Scientific Investigation in Xinjiang, grant No. 2021xjkk1001; Program of National Social Science Foundation of China, grant No. 22BJL061; Major Project of Xinjiang Social Science Foundation, grant No. 21AZD008; The National Natural Science Foundation of China, grant No. 41461035.

Data Availability Statement: The authors do not have permission to share data.

Conflicts of Interest: The authors declare no conflicts of interest.

References

1. United Nations The Sustainable Development Agenda—United Nations Sustainable Development. Available online: https://www.un.org/sustainabledevelopment/development-agenda/ (accessed on 8 September 2023).
2. Henderson, J.V.; Storeygard, A.; Weil, D.N. Measuring Economic Growth from Outer Space. *Am. Econ. Rev.* **2012**, *102*, 994–1028. [CrossRef] [PubMed]
3. Chen, X.; Nordhaus, W.D. VIIRS Nighttime Lights in the Estimation of Cross-Sectional and Time-Series GDP. *Remote Sens.* **2019**, *11*, 1057. [CrossRef]
4. Gu, H.; Chen, C.; Lu, Y.; Chu, Y.; Ma, Y. Construction of Regional Economic Development Model Based on Remote Sensing Data. *IOP Conf. Ser. Earth Environ. Sci.* **2019**, *310*, 052060. [CrossRef]
5. Bartik, T. *Evaluating the Impacts of Local Economic Development Policies on Local Economic Outcomes: What Has Been Done and What Is Doable?* W.E. Upjohn Institute for Employment Research: Kalamazoo, MI, USA, 2002.
6. Li, B.; Lu, S. Labor Education, Cash Transfers and Student Development: Evidence from China. *Int. Rev. Financ. Anal.* **2023**, *87*, 102565. [CrossRef]
7. Rising, J.A.; Taylor, C.; Ives, M.C.; Ward, R.E.T. Challenges and Innovations in the Economic Evaluation of the Risks of Climate Change. *Ecol. Econ.* **2022**, *197*, 107437. [CrossRef]
8. Wan, G.; Hu, X.; Liu, W. China's Poverty Reduction Miracle and Relative Poverty: Focusing on the Roles of Growth and Inequality. *China Econ. Rev.* **2021**, *68*, 101643. [CrossRef]
9. Wang, J.; Wei, X.; Guo, Q. A Three-Dimensional Evaluation Model for Regional Carrying Capacity of Ecological Environment to Social Economic Development: Model Development and a Case Study in China. *Ecol. Indic.* **2018**, *89*, 348–355. [CrossRef]
10. Yang, Y.; Liu, Y. The Code of Targeted Poverty Alleviation in China: A Geography Perspective. *Geogr. Sustain.* **2021**, *2*, 243–253. [CrossRef]
11. Jiang, L.; Kuijsten, A. Regional disparities of urbanization levels in China. *Chin. J. Popul. Sci.* **2001**, *1*, 45–51. (In Chinese)
12. Chen, Q.; Ye, T.; Zhao, N.; Ding, M.; Ouyang, Z.; Jia, P.; Yue, W.; Yang, X. Mapping China's Regional Economic Activity by Integrating Points-of-Interest and Remote Sensing Data with Random Forest. *Environ. Plan. B Urban Anal. City Sci.* **2021**, *48*, 1876–1894. [CrossRef]
13. Ivković, A. Limitations of the GDP as a measure of progress and well-being. *Ekonomski Vjesnik* **2016**, *29*, 257–272.
14. Kinyondo, A.; Pelizzo, R. Poor Quality of Data in Africa: What Are the Issues? *Politics Policy* **2018**, *46*, 851–877. [CrossRef]
15. Brock, G. A Remote Sensing Look at the Economy of a Russian Region (Rostov) Adjacent to the Ukrainian Crisis. *J. Policy Model.* **2019**, *41*, 416–431. [CrossRef]
16. Chen, D.; Zhang, Y.; Yao, Y.; Hong, Y.; Guan, Q.; Tu, W. Exploring the Spatial Differentiation of Urbanization on Two Sides of the Hu Huanyong Line—Based on Nighttime Light Data and Cellular Automata. *Appl. Geogr.* **2019**, *112*, 102081. [CrossRef]
17. Lin, J.; Luo, S.; Huang, Y. Poverty Estimation at the County Level by Combining LuoJia1-01 Nighttime Light Data and Points of Interest. *Geocarto Int.* **2022**, *37*, 3590–3606. [CrossRef]
18. Shao, Z.; Li, X. Multi-Scale Estimation of Poverty Rate Using Night-Time Light Imagery. *Int. J. Appl. Earth Obs. Geoinf.* **2023**, *121*, 103375. [CrossRef]
19. Wan, N.; Du, Y.; Liang, F.; Yi, J.; Qian, J.; Tu, W.; Huang, S. Nighttime Light Satellite Images Reveal Uneven Socioeconomic Development along China's Land Border. *Appl. Geogr.* **2023**, *152*, 102899. [CrossRef]
20. Zhao, N.; Cao, G.; Zhang, W.; Samson, E.L. Tweets or Nighttime Lights: Comparison for Preeminence in Estimating Socioeconomic Factors. *ISPRS J. Photogramm. Remote Sens.* **2018**, *146*, 1–10. [CrossRef]
21. Cao, C.; Zhang, B.; Xia, F.; Bai, Y. Exploring VIIRS Night Light Long-Term Time Series with CNN/SI for Urban Change Detection and Aerosol Monitoring. *Remote Sens.* **2022**, *14*, 3126. [CrossRef]

22. Chen, T.-H.K.; Prishchepov, A.V.; Fensholt, R.; Sabel, C.E. Detecting and Monitoring Long-Term Landslides in Urbanized Areas with Nighttime Light Data and Multi-Seasonal Landsat Imagery across Taiwan from 1998 to 2017. *Remote Sens. Environ.* **2019**, *225*, 317–327. [CrossRef]
23. Gibson, J.; Olivia, S.; Boe-Gibson, G.; Li, C. Which Night Lights Data Should We Use in Economics, and Where? *J. Dev. Econ.* **2021**, *149*, 102602. [CrossRef]
24. Li, G.; Fan, J.; Zhou, Y.; Zhang, Y. Development Characteristics Estimation of Shandong Peninsula Urban Agglomeration Using VIIRS Night Light Data. *Remote Sens. Technol. Appl.* **2021**, *35*, 1348–1359.
25. Li, X.; Xu, H.; Chen, X.; Li, C. Potential of NPP-VIIRS Nighttime Light Imagery for Modeling the Regional Economy of China. *Remote Sens.* **2013**, *5*, 3057–3081. [CrossRef]
26. Puri, P.; Puri, V. Observing Economics through Geography: COVID-19 and Night-Light Data Analysis of Bangladesh and Sri Lanka (2017–2021). *ACADEMICIA Int. Multidiscip. Res. J.* **2022**, *12*, 42–54. [CrossRef]
27. Tan, M.; Li, X.; Li, S.; Xin, L.; Wang, X.; Li, Q.; Li, W.; Li, Y.; Xiang, W. Modeling Population Density Based on Nighttime Light Images and Land Use Data in China. *Appl. Geogr.* **2018**, *90*, 239–247. [CrossRef]
28. Sutton, P.C.; Costanza, R. Global Estimates of Market and Non-Market Values Derived from Nighttime Satellite Imagery, Land Cover, and Ecosystem Service Valuation. *Ecol. Econ.* **2002**, *41*, 509–527. [CrossRef]
29. Wang, X.; Rafa, M.; Moyer, J.D.; Li, J.; Scheer, J.; Sutton, P. Estimation and Mapping of Sub-National GDP in Uganda Using NPP-VIIRS Imagery. *Remote Sens.* **2019**, *11*, 163. [CrossRef]
30. Li, D.; Li, X. An Overview on Data Mining of Nighttime Light Remote Sensing. *Acta Geod. Et Cartogr. Sin.* **2015**, *44*, 591–601. [CrossRef]
31. Li, C.; Huo, Z.; Wang, X.; Wu, Y. Study on Spatio-Temporal Modelling between NPP-VIIRS Night-Time Light Intensity and GDP for Major Urban Agglomerations in China. *Int. J. Remote Sens.* **2022**, 1–24. [CrossRef]
32. Chen, Z.; Yu, B.; Yang, C.; Zhou, Y.; Yao, S.; Qian, X.; Wang, C.; Wu, B.; Wu, J. An Extended Time Series (2000–2018) of Global NPP-VIIRS-like Nighttime Light Data from a Cross-Sensor Calibration. *Earth Syst. Sci. Data* **2021**, *13*, 889–906. [CrossRef]
33. Liang, H.; Guo, Z.; Wu, J.; Chen, Z. GDP Spatialization in Ningbo City Based on NPP/VIIRS Night-Time Light and Auxiliary Data Using Random Forest Regression. *Adv. Space Res.* **2020**, *65*, 481–493. [CrossRef]
34. Shi, K.; Yu, B.; Huang, Y.; Hu, Y.; Yin, B.; Chen, Z.; Chen, L.; Wu, J. Evaluating the Ability of NPP-VIIRS Nighttime Light Data to Estimate the Gross Domestic Product and the Electric Power Consumption of China at Multiple Scales: A Comparison with DMSP-OLS Data. *Remote Sens.* **2014**, *6*, 1705–1724. [CrossRef]
35. Li, X.; Ma, R.; Zhang, Q.; Li, D.; Liu, S.; He, T.; Zhao, L. Anisotropic Characteristic of Artificial Light at Night–Systematic Investigation with VIIRS DNB Multi-Temporal Observations. *Remote Sens. Environ.* **2019**, *233*, 111357. [CrossRef]
36. Goodchild, M.F. Citizens as Sensors: The World of Volunteered Geography. *GeoJournal* **2007**, *69*, 211–221. [CrossRef]
37. See, L.; Mooney, P.; Foody, G.; Bastin, L.; Comber, A.; Estima, J.; Fritz, S.; Kerle, N.; Jiang, B.; Laakso, M.; et al. Crowdsourcing, Citizen Science or Volunteered Geographic Information? The Current State of Crowdsourced Geographic Information. *ISPRS Int. J. Geo-Inf.* **2016**, *5*, 55. [CrossRef]
38. Goodchild, M.F.; Li, L. Assuring the Quality of Volunteered Geographic Information. *Spat. Stat.* **2012**, *1*, 110–120. [CrossRef]
39. Feige, E.L.; Urban, I. Measuring Underground (Unobserved, Non-Observed, Unrecorded) Economies in Transition Countries: Can We Trust GDP? *J. Comp. Econ.* **2008**, *36*, 287–306. [CrossRef]
40. Jokar Arsanjani, J.; Mooney, P.; Zipf, A.; Schauss, A. Quality Assessment of the Contributed Land Use Information from OpenStreetMap Versus Authoritative Datasets. In *OpenStreetMap in GIScience: Experiences, Research, and Applications*; Jokar Arsanjani, J., Zipf, A., Mooney, P., Helbich, M., Eds.; Lecture Notes in Geoinformation and Cartography; Springer International Publishing: Cham, Switzerland, 2015; pp. 37–58, ISBN 978-3-319-14280-7.
41. Neis, P.; Zielstra, D. Recent Developments and Future Trends in Volunteered Geographic Information Research: The Case of OpenStreetMap. *Future Internet* **2014**, *6*, 76–106. [CrossRef]
42. Zheng, S.; Zheng, J. Assessing the Completeness and Positional Accuracy of OpenStreetMap in China. In *Thematic Cartography for the Society*; Bandrova, T., Konecny, M., Zlatanova, S., Eds.; Lecture Notes in Geoinformation and Cartography; Springer International Publishing: Cham, Switzerland, 2014; pp. 171–189, ISBN 978-3-319-08180-9.
43. Moradi, M.; Roche, S.; Mostafavi, M.A. Exploring Five Indicators for the Quality of OpenStreetMap Road Networks: A Case Study of Québec, Canada. *Geomatica* **2022**, *75*, 178–208. [CrossRef]
44. Barrington-Leigh, C.; Millard-Ball, A. Global Trends toward Urban Street-Network Sprawl. *Proc. Natl. Acad. Sci. USA* **2020**, *117*, 1941–1950. [CrossRef]
45. Hadimlioglu, I.A.; King, S.A. City Maker: Reconstruction of Cities from OpenStreetMap Data for Environmental Visualization and Simulations. *ISPRS Int. J. Geo-Inf.* **2019**, *8*, 298. [CrossRef]
46. Zhang, L.; Pfoser, D. Using OpenStreetMap Point-of-Interest Data to Model Urban Change—A Feasibility Study. *PLoS ONE* **2019**, *14*, e0212606. [CrossRef] [PubMed]
47. Herfort, B.; Lautenbach, S.; Porto de Albuquerque, J.; Anderson, J.; Zipf, A. The Evolution of Humanitarian Mapping within the OpenStreetMap Community. *Sci. Rep.* **2021**, *11*, 3037. [CrossRef] [PubMed]
48. Liu, B.; Shi, Y.; Li, D.-J.; Wang, Y.-D.; Fernandez, G.; Tsou, M.-H. An Economic Development Evaluation Based on the OpenStreetMap Road Network Density: The Case Study of 85 Cities in China. *ISPRS Int. J. Geo-Inf.* **2020**, *9*, 517. [CrossRef]

49. Borkowska, S.; Pokonieczny, K. Analysis of OpenStreetMap Data Quality for Selected Counties in Poland in Terms of Sustainable Development. *Sustainability* **2022**, *14*, 3728. [CrossRef]
50. Budhathoki, N.R. *Participants' Motivations to Contribute Geographic Information in an Online Community*; University of Illinois at Urbana-Champaign: Champaign, IL, USA, 2010; ISBN 1-124-58124-3.
51. Cheng, F.; Liu, S.; Hou, X.; Zhang, Y.; Dong, S.; Coxixo, A.; Liu, G. Urban Land Extraction Using DMSP/OLS Nighttime Light Data and OpenStreetMap Datasets for Cities in China at Different Development Levels. *IEEE J. Sel. Top. Appl. Earth Obs. Remote Sens.* **2018**, *11*, 2587–2599. [CrossRef]
52. Shi, L.; Ling, F. Local Climate Zone Mapping Using Multi-Source Free Available Datasets on Google Earth Engine Platform. *Land* **2021**, *10*, 454. [CrossRef]
53. Wang, L.; Fan, H.; Wang, Y. An Estimation of Housing Vacancy Rate Using NPP-VIIRS Night-Time Light Data and OpenStreetMap Data. *Int. J. Remote Sens.* **2019**, *40*, 8566–8588. [CrossRef]
54. Ma, D.; Guo, R.; Jing, Y.; Zheng, Y.; Zhao, Z.; Yang, J. Intra-Urban Scaling Properties Examined by Automatically Extracted City Hotspots from Street Data and Nighttime Light Imagery. *Remote Sens.* **2021**, *13*, 1322. [CrossRef]
55. Griffith, D.A.; Arbia, G. Detecting Negative Spatial Autocorrelation in Georeferenced Random Variables. *Int. J. Geogr. Inf. Sci.* **2010**, *24*, 417–437. [CrossRef]
56. Anselin, L.; Syabri, I.; Kho, Y. GeoDa: An Introduction to Spatial Data Analysis. In *Handbook of Applied Spatial Analysis: Software Tools, Methods and Applications*; Fischer, M.M., Getis, A., Eds.; Springer: Berlin/Heidelberg, Germany, 2010; pp. 73–89, ISBN 978-3-642-03647-7.
57. Wu, Y.; Zhu, X.; Gao, W.; Qian, F. The Spatial Characteristics of Coupling Relationship between Urbanization and Eco-Environment in the Pan Yangtze River Delta. *Energy Procedia* **2018**, *152*, 1121–1126. [CrossRef]
58. Li, C.; Wu, K.; Gao, X. Manufacturing Industry Agglomeration and Spatial Clustering: Evidence from Hebei Province, China. *Environ. Dev. Sustain.* **2020**, *22*, 2941–2965. [CrossRef]
59. Moran, P.A.P. Notes on Continuous Stochastic Phenomena. *Biometrika* **1950**, *37*, 17–23. [CrossRef] [PubMed]
60. Anselin, L. Local Indicators of Spatial Association—LISA. *Geogr. Anal.* **1995**, *27*, 93–115. [CrossRef]
61. Ord, J.K.; Getis, A. Local Spatial Autocorrelation Statistics: Distributional Issues and an Application. *Geogr. Anal.* **1995**, *27*, 286–306. [CrossRef]
62. Qiu, M.; Zuo, Q.; Wu, Q.; Yang, Z.; Zhang, J. Water Ecological Security Assessment and Spatial Autocorrelation Analysis of Prefectural Regions Involved in the Yellow River Basin. *Sci. Rep.* **2022**, *12*, 5105. [CrossRef] [PubMed]
63. Huang, B.; Wu, B.; Barry, M. Geographically and Temporally Weighted Regression for Modeling Spatio-Temporal Variation in House Prices. *Int. J. Geogr. Inf. Sci.* **2010**, *24*, 383–401. [CrossRef]
64. Yu, D. Understanding Regional Development Mechanisms in Greater Beijing Area, China, 1995–2001, from a Spatial–Temporal Perspective. *GeoJournal* **2014**, *79*, 195–207. [CrossRef]
65. Yu, D.; Lv, B. Challenging the Current Measurement of China's Provincial Total Factor Productivity: A Spatial Econometric Perspective. *China Soft Sci.* **2009**, *11*, 160–170.
66. Li, W.; Ji, Z.; Dong, F. Spatio-Temporal Evolution Relationships between Provincial CO_2 Emissions and Driving Factors Using Geographically and Temporally Weighted Regression Model. *Sustain. Cities Soc.* **2022**, *81*, 103836. [CrossRef]
67. Akaike, H. Information Theory and an Extension of the Maximum Likelihood Principle. In *Selected Papers of Hirotugu Akaike*; Parzen, E., Tanabe, K., Kitagawa, G., Eds.; Springer Series in Statistics; Springer: New York, NY, USA, 1998; pp. 199–213, ISBN 978-1-4612-1694-0.
68. Hu, H.Y. The Distribution of Population in China, with Statistics and Maps. *Acta Geogr. Sin.* **1935**, *2*, 33–74. [CrossRef]
69. Gao, J.; Li, S. Detecting Spatially Non-Stationary and Scale-Dependent Relationships between Urban Landscape Fragmentation and Related Factors Using Geographically Weighted Regression. *Appl. Geogr.* **2011**, *31*, 292–302. [CrossRef]
70. Boscolo, D.; Paul Metzger, J. Isolation Determines Patterns of Species Presence in Highly Fragmented Landscapes. *Ecography* **2011**, *34*, 1018–1029. [CrossRef]
71. Gao, Y.; Huang, J.; Li, S.; Li, S. Spatial Pattern of Non-Stationarity and Scale-Dependent Relationships between NDVI and Climatic Factors—A Case Study in Qinghai-Tibet Plateau, China. *Ecol. Indic.* **2012**, *20*, 170–176. [CrossRef]
72. Auxier, B.; Anderson, M. *Social Media Use in 2021*; Pew Research Center: Washington, DC, USA, 2021; Volume 1, pp. 1–4.
73. Bimber, B. Measuring the Gender Gap on the Internet. *Soc. Sci. Q.* **2000**, *81*, 868–876.
74. Calvert, S.L.; Rideout, V.J.; Woolard, J.L.; Barr, R.F.; Strouse, G.A. Age, Ethnicity, and Socioeconomic Patterns in Early Computer Use: A National Survey. *Am. Behav. Sci.* **2005**, *48*, 590–607. [CrossRef]
75. Song, Y.; Li, X.; Tao, G.; Liu, J. Exploring the Characteristics and Drivers of Expansion in the Shandong Peninsula Urban Agglomeration Based on Nighttime Light Data. *IEEE J. Sel. Top. Appl. Earth Obs. Remote Sens.* **2023**, *16*, 8535–8549. [CrossRef]
76. Xu, G.; Su, J.; Xia, C.; Li, X.; Xiao, R. Spatial Mismatches between Nighttime Light Intensity and Building Morphology in Shanghai, China. *Sustain. Cities Soc.* **2022**, *81*, 103851. [CrossRef]
77. Yang, Z.; Chen, Y.; Guo, G.; Zheng, Z.; Wu, Z. Using Nighttime Light Data to Identify the Structure of Polycentric Cities and Evaluate Urban Centers. *Sci. Total Environ.* **2021**, *780*, 146586. [CrossRef]
78. Li, S.; Zhang, T.; Yang, Z.; Li, X.; Xu, H. Night time light satellite data for evaluating the socioeconomics in central Asia. *Int. Arch. Photogramm. Remote Sens. Spatial Inf. Sci.* **2017**, *42*, 1237–1243. [CrossRef]

79. Huang, Z.; Li, S.; Gao, F.; Wang, F.; Lin, J.; Tan, Z. Evaluating the Performance of LBSM Data to Estimate the Gross Domestic Product of China at Multiple Scales: A Comparison with NPP-VIIRS Nighttime Light Data. *J. Clean. Prod.* **2021**, *328*, 129558. [CrossRef]
80. Cui, Y.; Shi, K.; Jiang, L.; Qiu, L.; Wu, S. Identifying and Evaluating the Nighttime Economy in China Using Multisource Data. *IEEE Geosci. Remote Sens. Lett.* **2021**, *18*, 1906–1910. [CrossRef]
81. Wong, D.W.S. The Modifiable Areal Unit Problem (MAUP). In *WorldMinds: Geographical Perspectives on 100 Problems: Commemorating the 100th Anniversary of the Association of American Geographers 1904–2004*; Janelle, D.G., Warf, B., Hansen, K., Eds.; Springer: Dordrecht, The Netherlands, 2004; pp. 571–575, ISBN 978-1-4020-2352-1.
82. Encalada-Abarca, L.; Ferreira, C.C.; Rocha, J. Measuring Tourism Intensification in Urban Destinations: An Approach Based on Fractal Analysis. *J. Travel Res.* **2022**, *61*, 394–413. [CrossRef]
83. Long, Y.; Zhai, W.; Shen, Y.; Ye, X. Understanding Uneven Urban Expansion with Natural Cities Using Open Data. *Landsc. Urban Plan.* **2018**, *177*, 281–293. [CrossRef]